Evaluation and Comparison of Structurally Different Cellulose-Based Hemostatic Agents in a Rat Kidney Model

Alice Paprskářová
Veterinární a farmaceutická univerzita Brno: Veterinarni a farmaceuticka univerzita Brno
Pavel Suchy (suchypa@pharm.muni.cz)
Masarykova univerzita Farmaceutická fakulta Brno Jihomoravský CZ https://orcid.org/0000-0002-6277-2749
Marta Chalupová
Masaryk University: Masarykova Univerzita
Lenka Michlovská
VUT: Vysoke uceni technicke v Brne
Jarmila Klusáková
Masarykova Univerzita
Tomáš Sopuch
Holzbecher s.r.o.
Lucy Vojtová
VUT: Vysoke uceni technicke v Brne

Research Article

Keywords: hemostasis, partial nephrectomy, sponge, nonwoven textile, knitted fabric, rat

Posted Date: March 11th, 2021

DOI: https://doi.org/10.21203/rs.3.rs-255272/v1

Version of Record: A version of this preprint was published at Cellulose on August 6th, 2021. See the published version at https://doi.org/10.1007/s10570-021-04104-1.

Abstract

Different topical hemostatic materials are used to achieve effective hemostasis. High hemostatic activity, biocompatibility, bioresorbability, and easy manipulation are to be expected in such a developed product. In the surgical world with these specific requirements, finding a proper hemostatic agent is very difficult. The study compared several materials of various construction properties, which were assessed for structural and related properties by morphological analyses and assessed *in vivo* for their efficiency and behaviour using a model of rat partial nephrectomy. New sodium salt of carboxymethyl cellulose (CMC) sponge with the lowest porosity and free swell absorptive capacity contained the highest amount of hydroxyl and carboxyl groups. Results revealed that this CMC material in the form of a bioresorbable sponge may ensure the necessary hemostatic effects, while also providing a positive influence on the reaction of the local tissue. The CMC material also needed significantly less time to achieve hemostasis ($p < 0.001$). Moreover, the sponge reached satisfactory results in the histopathological evaluation with the lowest destruction score and favorable healing reaction. This modified product proved itself to be a promising bioresorbable hemostat, which, according to its design, matches with its surgical applications. In general, the obtained data elucidated the dependency of the total effect on its structure and composition.

Introduction

In the field of surgery, different techniques are used to achieve fast and efficient hemostasis, particularly in urological surgical procedures requiring new mechanisms for controlled bleeding (Samudrala 2008). Physical methods are not always successful in these cases. Thermal modalities may increase the risk of infection, causing an undesirable inflammatory reaction as well as tissue necrosis (Hassouna and Manikandan 2012; Ikehara et al. 2015). That is why many new hemostats have come to the fore in surgical research. Various hemostatic materials have different specific features, therefore they cannot be used universally (Achneck et al. 2010). New local hemostats are continuously developed and it is necessary to prove their potential effect on a suitable model. It is important to stop any bleeding and to influence positively the regeneration of the damaged tissue as well as to contribute to the fast healing of the wound without any complications. There is a strong effort to create a safe bioresorbable material with all above-mentioned features, and which would be easy to manipulate. The most commonly used local hemostats have been the same for several decades: gelatine foam, bone wax, fibrillar collagen, and several derivatives of cellulose (Schonauer et al. 2004). Oxidized regenerated cellulose has been traditionally used as a hemostat for more than 60 years (Zhang et al. 2020). Its biodegradability and antibacterial properties represent the main advantage (Spangler et al. 2003; Wu et al. 2018). However, hemostatic materials based on carboxymethyl cellulose (CMC) have recently been introduced to the market as well. Current studies describe also other new types of hemostatic materials that are being used, e.g. modified sodium starch glycolate (Panwar et al. 2020); a new tissue factor-based topical hemostat TT-173 (Centeno et al. 2020); recombinant topical thrombin with a gelatine sponge carrier (Slezak et al. 2020). Until now, there has been a recent trend to innovate and improve upon standard dressings and techniques. Composite materials based on carboxymethyl cellulose and collagen are not widespread yet. Exploration of collagen properties and different types of cellulose may enable the creation of other medically useful materials.

This study aimed to evaluate newly modified hemostatic materials using a nephrectomy model in rats. Experiments focused on the local reaction of the renal parenchyma to hemostatic materials that have the ability to effectively stop extensive bleeding and that contribute to the normal healing process, with special consideration for the required histopathological parameters.

Materials And Methods

Hemostatic Materials

Hemostatic materials of three different textile structures (spunlace, needle-punched, and knitted) were prepared for the assessment. Needle-punched textiles and spunlace textiles, as representatives of nonwoven fabrics, differ in the reinforcement of fibers. Needle punching is mediated by mechanical needle reinforcement. The spunlace textile, characterized by a web of entangled fibers, is prepared during the process of hydroentanglement that uses a high pressure water jet. These two above-mentioned textiles are created from separate fibers, contrary to knitted structures made of yarns formed into loops. Each material offers specific capabilities and therefore is designed for different medical applications. Spunlace materials possess very good strength. Nonwoven textiles, mainly of needle-punched type, should be more reactive. Their structure based on free fibers is easily accessible and can therefore absorb more medium. On the other hand, knitted materials have lower absorption capacity. Their advantage is in the flexibility of such a material. Sponges, such as freeze-dried three-dimensional structures, were also evaluated in the experiment. The process of lyophilization improves the absorption ability and therefore enables combining different polymers. Carboxymethyl cellulose can be processed into all aforementioned structures.

All tested materials were based on different cellulose derivatives. Oxidized regenerative cellulose was chosen as the control agent (ORC fibril, areal weight 37 $g.m^{-2}$). The first evaluated preparation consisted of sodium salt of carboxymethyl cellulose from Tencel fibers in the form of needle-punched nonwoven textile (CMC Na needle-punched, areal weight 138.3 $g.m^{-2}$). The degree of substitution of the textile was 0.335 and the pH was 6.13. Another material was based on acidic carboxymethyl cellulose (CMC H-spunlace, areal weight 80 $g.m^{-2}$). The form was prepared by carboxymethylation of cotton spunlace textile. The material was characterized by the degree of substitution 0.39 and the pH was 3.5. As the next agent, we assessed another needle-punched nonwoven textile prepared by mixing polypropylene and viscose fibers (PP/Vis needle-punched, 15% PP and 85% Vis, areal weight 330 $g.m^{-2}$). Another tested material was a commercial sample of soluble hemostatic gauze, knit based on the sodium salt of regenerated carboxymethyl cellulose with a degree of substitution 0.725 (CMC Na knit, areal weight 331.7 $g.m^{-2}$). So called biosoluble hemostats made of sodium salt of carboxymethyl cellulose represent relatively new products coming from China. Contrary to the oxidized regenerated cellulose, which is commonly used in its acidic form, these hemostats have neutral pH creating a sticky gelling substances in contact with blood. The knit was also modified and used in its acidic form of carboxymethyl cellulose (CMC H knit, areal weight 312.6 $g.m^{-2}$). The lyophilized sodium salt of the carboxymethyl cellulose version of the mentioned soluble hemostatic gauze - prepared as a sponge by freeze-drying (Christ Epsilon 2 10D LSCPlus, -35 °C, 15 Pa, 48 h) was also assessed (CMC Na sponge, areal weight 360.2 $g.m^{-2}$). Lastly, we evaluated lyophilized carboxymethyl cellulose sodium salt with the addition of 5% collagen in sponge form prepared by combining soluble hemostatic gauze and bovine collagen type I (CMC Na/Coll sponge, areal weight 409 $g.m^{-2}$). For better clarity, all tested materials are described in Table 1.

Table 1 Summary of all tested materials, their composition and form

Sample	Base	Structural design
CMC Na sponge	Carboxymethyl cellulose sodium salt	Sponge
CMC Na/Coll sponge	Carboxymethyl cellulose sodium salt + collagen	Sponge
CMC Na knit	Regenerated carboxymethyl cellulose sodium salt	Knitted structure
CMC H knit	Carboxymethyl cellulose acidic form	Knitted structure
PP/Vis needle-punched	Polypropylene + viscose	Needle-punched nonwoven textile
CMC Na needle-punched	Carboxymethyl cellulose sodium salt	Needle-punched nonwoven textile
CMC H spunlace	Carboxymethyl cellulose acidic form	Spunlace form of nonwoven textile
ORC fibril	Regenerated oxidized cellulose	Fibrillar structure (similar to needle-punched)

Animal Model

The work described has been carried out in accordance with all required guidelines for animal experiments. At first, the Scientific Committee for the Protection of Animals at university approved the whole *in vivo* concept. A partial nephrectomy model in rats was then performed (Chalupová et al. 2012; Suchý et al. 2020). 80 male Wistar laboratory rats (AnLab, Czech Republic) with an average weight of 265 ± 62 g were randomly divided into 8 groups of 10 animals. The rats were placed in an air-controlled room with free access to water and standard laboratory feed. These animals were anesthetized by i.m. administration of a mixture composed of tiletamine and zolazepam (Zoletil 100, Virbac S A., France). A dose of 65 $mg.kg^{-1}$ was applied. Next, the peritoneum was surgically opened and a partial-nephrectomy of the left kidney's caudal pole was undertaken. Immediately after this intervention, 1 cm^2 pieces of the tested hemostatic materials were applied directly to the bleeding wound and the time for hemostasis completion was measured. The hilar structures were not ligated. Once hemostasis was achieved, the hemostatic agent remained on the wound. The injured kidney was placed back in the peritoneal cavity. Both the peritoneum and skin were then sutured. One half of the animals from each group were euthanized 3 days after the intervention using inhalation anesthesia isoflurane (Forane, Aesica Queenborough Ltd., Kent). The remaining half was euthanized after 30 days in the same manner. The condition of the peritoneal cavity was evaluated during the necropsy and one section of the left kidney was collected for histopathological evaluation. Prepared tissue samples were fixed in formalin, embedded in paraffin, and stained with hematoxylin and eosin.

Monitored Parameters

The morphology of all aforementioned materials was analyzed by a scanning electron microscope (SEM), Tescan MIRA3 (Tescan, Czech Republic). In order to achieve better resolution, the samples were covered by a 20 nm gold/palladium layer. All samples were measured using secondary emission mode and depth regime with 10 kV acceleration mode. Studying the SEM images, the porosity of all tested materials was calculated by using ImageJ software (Java version). The free swell absorptive capacity was determined gravimetrically according to the standard ČSN EN 13726-1 for medical devices. As a liquid medium, 8.3 g of sodium chloride and 0.28 g of calcium dichloride in 1000 ml solution were used. Free swelling capacity was calculated using eq. 1:

$$\text{Free swell absorptive capacity} = \frac{W_t - W_0}{W_0} \quad (1)$$

where w_0 is the weight of dry sample and w_t is the weight of wet sample after 30 min. Materials were also assessed by their attenuated total reflection – Fourier transform infrared spectroscopy (ATR-FTIR spectroscopy). It was used to compare the chemical structure of the hemostatic agents. Samples were measured as they were received in the original hemostatic form. ATR-FTIR spectra were obtained with a Hyperion 3000/Vertex 70V (Bruker) with an average of 64 scans in the spectral range of 4000 – 400 cm^{-1} using software Opus 7.5.

The hemostatic agent was applied to the open wound during the *in vivo* experiment. Time to hemostasis completion was measured in seconds. A complete histopathological evaluation provided information about the local tissue reaction. A histological examination followed several parameters: tissue destruction at the site of damage (D), extent of fibroproduction (F), reaction of the surrounding tissue (R) and inflammatory infiltration (I). These parameters were evaluated on the following scale: 0 (insignificant or just a light presence of the given parameter), 1 (medium presence), 2 (very significant presence). For more accuracy, half points on the scale were used. The total destruction score was calculated as the sum of the detected values. The lowest score showed the best result. For the first parameter (D), mainly the extent of necrosis and destructive bleeding were viewed. For the second parameter (F), excessive fibroproduction, which appears as an indication of undesirable irritation, was monitored. The tissue surrounding the wound was examined for any reaction, as per the third parameter (R). In particular, dystrophic changes of the epithelium of the renal tubules and the presence of protein and hemoglobin cylinders in them were observed for the intensity and extent of inflammatory infiltration (I).

Statistical Analysis

Hemostatic data showed heterogeneous variances. Data were subjected to a nonparametric Kruskal-Wallis statistical test for multiple comparisons using Statistica 10 software (StatSoft, Czech Republic) accordingly. Statistically significant differences were compared between all analyzed groups. Data were expressed as means ± standard deviation.

Results

Prior hemostasis evaluation, both the chemical structure and morphology of the used hemostatic materials were analyzed since these parameters are crucial for the hemostasis efficiency.

Chemical Composition

The results of ATR-FTIR spectroscopy spectra comparing the chemical structure of the used hemostats are shown in Fig. 1. The ATR-FTIR spectrum of the controlled ORC fibril (blue line) displayed a small broad absorption band of approx. 3600 to 3000 cm^{-1} that belonged to the stretching vibration of the hydroxyl –OH groups. This broad band was more visible in CMC samples, while the largest was represented by the CMC Na sponge (pink line). Interestingly, no band was visible in this region in the PP/Vis needle-punched sample (black line). However, this sample did show the largest bands at 2918 and 2848 cm^{-1}, confirming the C–H stretching vibration of the $–CH_2$ polypropylene groups. The band that resulted from the ring stretching of glucose appeared at 1611 cm^{-1} at CMC samples. The bands at 1434 and 1340 cm^{-1} included $–CH_2$ scissoring and C–OH bending vibrations, respectively. The band at 1160 cm^{-1} was assigned to the asymmetric vibration of the glycosidic bonds in cellulose molecules. Very strong absorption bands at 1058 and 1028 cm^{-1} were attributed to skeletal vibrations involving the stretching of C–O and C–C bonds, respectively, that are attached to the glucose rings. The weak bands at approximately 720 cm^{-1} were due to ring stretching and ring deformation of α-D-(1–4) and α-D-(1–6) linkages (El-Sakhawy et al. 2000; Fukuzumi et al. 2010; Wang et al. 2005). To conclude, the highest

variant was the PP/Vis needle-punched sample affected by the polypropylene network. The largest number of both hydroxyl and carboxyl groups showed samples CMC (CMC Na sponge - pink line and CMC Na/Coll sponge – orange line), while CMC H spunlace (violet line) was the most chemically similar to control ORC fibril (blue line).

Morphology of Hemostats

In addition to the chemical composition, the size and shape are other important factors that determine the properties of functional materials. As shown SEM images in Fig. 2, the structure of used hemostatic materials was very different. Samples a) (CMC Na sponge) and b) (CMC Na/coll sponge) were porous foams prepared by freeze-drying. Interconnected pores permitted fast liquid absorption. Very similar was the structure of knitted fabrics of sample c) (CMC Na knit) and d) (CMC H knit) - CMC H knit was actually acidic form made of CMC Na knit, where sample c) was scanned from the top and sample d) from the bottom. Other samples e) (PP/Vis n-punched), f) (CMC Na n-punched) g) (CMC H spunlace) and h) (ORC fibril) yielded very similar fibrilar morphology, where just sample e) had a significant PP network on the surface of viscose, probably due to better mechanical properties and manipulation. Porosity of the materials was determined and the results are shown in Table 2. The highest porosity was found out for CMC Na/Coll sponge followed by CMC Na knit. Other materials revealed lower porosity. Interestingly, the absolutely lowest porosity of all materials was calculated at CMC Na sponge. Absorption capacity was determined as well. Results are shown in Fig. 3. Sponges followed by knits had the lowest free swell absorptive capacity.

Table 2 Porosity of hemostatic materials

Sample	Porosity (%)
CMC Na sponge	7.6
CMC Na/Coll sponge	72.8
CMC Na knit	49.9
CMC H knit	22.1
PP/Vis needle-punched	11.8
CMC Na needle-punched	27.6
CMC H spunlace	20.3
ORC fibril	20.6

Time to Hemostasis

The bleeding was completely stopped before the peritoneum was closed again. No animal bled to death immediately after the surgery or during the convalescence period. We recorded significantly shorter time to hemostasis in the CMC Na sponge (6.1 ± 3.7 s), the CMC Na/Coll sponge (6.8 ± 3.5 s) and the CMC Na knit (9.5 ± 4.2 s) compared to the control ORC fibril (34.6 ± 9.5 s). Both sponges also reached significantly less time than the CMC Na needle-punched (28.5 ± 7.8 s), the CMC H spunlace (28.6 ± 9.5 s) and the PP/Vis needle-punched (23.8 ± 7.3 s). The CMC Na knit proved to have significantly better hemostatic effect compared to the CMC Na needle-punched and the CMC H spunlace. The results with the observed statistically significant differences are summarized in the graph in Fig. 4.

Necropsy and Macroscopic Findings

One half of the animals from each group were evaluated after 3 days. The remaining half was evaluated after 30 days.

In the CMC Na sponge, the material was completely absorbed in one case. Other cases revealed remnants of material with traces of blood in one rat. After 30 days, the material was completely absorbed. There was a pale-coloured kidney in one case and a substantial amount of fat around the intestine.

In the CMC Na/Coll sponge, the remaining material with traces of blood was observed on the wound at the 3-day evaluation. The 30-day assessment confirmed the bioresorbability of the material.

In the CMC Na knit, the material remained attached to the wound in one case. Other cases revealed bioresobability after 3 days. The kidney had a pale appearance in 3 rats. After 30 days, the kidneys looked healthy and there was no material remaining.

In the CMC H knit, the material transformed into a gel and remained on the wound after 3 days. After 30 days, the material was completely absorbed.

In the PP/Vis needle-punched, the material was stuck to the wound at the 3-day evaluation. The kidney had a pale look in one case. Although after 30 days the material remained on the wound, there were no signs of granulomatous reaction.

In the CMC Na needle-punched, the used material was stuck to the wound at both evaluation periods. Granulomatous reaction prevailed in most cases of the 30-day evaluation. There was a significant abscessing inflammation, particularly in one rat in this assessment.

In the CMC H spunlace, the material was still on the wound at the 3-day evaluation. There was one pale kidney and a trace amount of ascites. After 30 days, the material remained in the rat's body. There were signs of granulomatous reaction in most cases. An icteral colour of fat around the kidney was registered in one rat.

In the ORC fibril, the remaining material was observed on the wound after 3 days. The tested material adhered to the wound and revealed traces of blood. The manufacturer has guaranteed the bioresorbability after 7-14 days. Therefore, the assessment after 30 days was a decisive aspect for us and it confirmed the bioresorbability of the material. One pale kidney was detected in a tested rat. The finding may be attributed to a more extensive blood loss. The remaining kidneys retained a healthy appearance.

Histopathological Evaluation

All monitored histopathological features are summarized in Table 3. The total destruction score revealed a direct influence on the healing tissue. The group with the lowest number was thus considered the most suitable material of this study.

Table 3 Histopathological evaluation after 3(a) and 30(b) days. Followed parameters: D, tissue destruction; F, extent of fibroproduction; R, reaction of the surrounding tissue; I, inflammatory infiltration

		Evaluated parameters				
	Resorbability	D	F	R	I	Destruction score
CMC Na sponge[a]	no	1,1,1,0.5,1	1,0.5,0.5,0.5,0.5	1,0.5,0.5,0.5,0.5	1,0.5,0.5,0.5,1	14
CMC Na/Coll sponge[a]	no	1.5,1,1.5,1,1.5	1,0.5,1,1,1	1.5,1.5,1.5,1,0.5	1.5,1,1.5,1,1	23
CMC Na knit[a]	yes	0.5,1.5,1.5,1.5,1	0.5,1,1,1,1	0.5,1.5,1.5,1,1	0.5,1,1,1,1	20.5
CMC H knit[a]	no	1,1,1,1,0.5	1,1,1,1,1	1,1,1,1,1	2,1.5,1.5,1,0.5	21
PP/Vis needle-punched[a]	no	1,1,1,1,1	1,0,0,1,1	1,2,1,1,1	1,1,1,1,2	20
CMC Na needle-punched[a]	no	1,1,1,2,1	1,1,1,1,1	1,2,2,2,1	1,1,1,1,1	24
CMC H spunlace[a]	no	2,1,1,1,2	1,1,1,1,0	2,1,2,2,2	2,1,1,1,1	26
ORC fibril[a]	no	2,1,2,2,1	1,1,1,1,1	1,1,1,1,2	1,1,1,1,2	25
CMC Na sponge[b]	yes	1,0.5,0.5,0.5,0.5	0.5,0.5,0.5,0.5,0	1,0.5,0.5,0.5,0.5	1,0.5,0.5,0.5,0.5	11
CMC Na/Coll sponge[b]	yes	0.5,1,0.5,1,1	0.5,1,0.5,1,1	0.5,0.5,0,1,1	0.5,1.5,0.5,2,1.5	17
CMC Na knit[b]	yes	1,0.5,1.5,1,0.5	1,1,0.5,1.5, 0.5	0.5,0.5,1,1,0	0.5,0.5,2,2,0	17
CMC H knit[b]	yes	0.5,0.5,0.5,0.5,1	0.5,0.5,0.5, 0.5,1	0.5,1,0.5,0.5,1.5	1,1,0.5,1,2	15.5
PP/Vis needle-punched[b]	no	2,1,1,0,1	1,0,1,0,0	1,1,1,1,1	1,0,1,0,1	15
CMC Na needle-punched[b]	no	1,2,0,1,1	2,2,2,2,2	1,2,1,1,1	2,2,0,2,2	29
CMC H spunlace[b]	no	1,2,2,1,1	2,2,2,2,2	1,1,2,2,1	2,2,2,2,2	34
ORC fibril[b]	yes	1,2,1,1,1	1,2,1,1,2	1,2,2,1,1	1,2,2,2,2	29

In the CMC Na sponge samples revealed small clear zones of inflammation and necrosis after 3 days (Fig. 5a). The destruction score was 14. A relatively favorable healing reaction appeared after 30 days. Almost clear cutting line with only a slight inflammatory reaction still occurred (Fig. 6a). The destruction score was 11. The CMC Na sponge had the best result considering both destruction scores.

In the CMC Na/Coll sponge samples showed massive inflammation and presence of necrosis after 3 days (Fig. 5b). The total destruction score was 23 after 3 days and 17 after 30 days. The evaluation after 30 days revealed the presence of granulomas, bleeding, and a clear area of inflammation (Fig. 6b).

In the CMC Na knit, samples were characterized by necrotic tissue. Renal tubules with massive inflammation around appeared in the preparations (Fig. 5c). The destruction score was 20.5 after 3 days. This score decreased after 30 days to number 17. After a longer period, the parenchyma showed very significant inflammation and the presence of granulomas (Fig. 6c).

The CMC H knit material caused complete destruction of the tissue by necrosis after 3 days. There was massive inflammation and signs of bleeding (Fig. 5d). The total destruction score was 21. The number decreased after 30 days to 15.5. A relatively narrow area of inflammation appeared after a longer period (Fig. 6d).

In the PP/Vis needle-punched, samples showed a smooth cutting line with the hematoma after 3 days. There were protein cylinders with significant reaction (Fig. 5e). The total destruction score was 20. The score decreased after 30 days to number 15. There was just a slight inflammatory reaction and subsequent scarring (Fig. 6e).

In the CMC Na needle-punched, samples were characterized by damaged tissue with protein cylinders and the clear sign of fibroproduction after 3 days (Fig. 5f). There was also the presence of a hematoma and thrombotic blood vessels in one case. The total destruction score was 24. The evaluation after 30 days revealed the rest of the material and inflammatory reaction with significant scarring (Fig. 6f). Finally, the total destruction score was 29.

In the CMC H spunlace, samples were characterized by fibroproduction after 3 days. The assessment revealed necrosis and inflammatory reaction around (Fig. 5g). The total destruction score was 26. The parenchyma was quite similar to the CMC Na needle-punched after 30 days. There was the rest of the material with significant formation of scar tissue (Fig. 6g). The total destruction score was 34. This material showed the worst effect on the tissue at all

After 3 days, in the ORC fibril, necrosis and dispersed inflammatory cells were revealed (Fig. 5h). The total destruction score was 25. After 30 days, the parenchyma showed signs of granulomatous reaction around the foreign material and chronic inflammatory infiltration (Fig. 6h). The total destruction score increased to 29.

Discussion

Various surgical procedures require specific hemostatic agents to get bleeding under control. In renal surgery especially, the requirements are more exacting and it is desirable to find a material that would be able to stop bleeding and improve tissue regeneration. All new hemostatic materials possess different characteristics. It is important to verify their therapeutic activity with a proper animal model even if it is just a new derivative of a previously introduced agent. Different animal models have been using for *in vivo* testing of hemorrhage. Parenchymatous organs such as the liver, spleen, and kidney are frequently used; one, because they bleed very easily and two, it is very difficult to control their bleeding, which may result in a serious life-threatening complication (Song et al. 2010).

One of the most common models is renal hemorrhage. The kidney accepts 1/5 of the cardiac output, so the renal parenchyma can easily bleed once it is injured and this accompanying bleeding can lead to serious consequences.

Therefore, in renal surgery it is necessary to use adequate hemostats (Huri et al. 2009; Ozgor et al. 2016).

The rat model of renal hemorrhage is still the simplest and appropriate method for the basic assessment of a hemostatic agent's effect together with its features and qualities. We also chose this model for testing. In the study, six materials based on carboxymethyl cellulose (CMC), derivatives with different types of structural modification (CMC Na needle-punched, CMC H spunlace, CMC Na/Coll sponge, CMC Na sponge, CMC Na knit, CMC H knit), and one non-carboxymethylated viscose derivative (PP/Vis needle-punched) were compared with the reference oxidized regenerated cellulose material (ORC fibril). In general, the ORC textile has a kind of privileged reputation among hemostats, so it can be considered as a better hemostatic agent than carboxymethyl cellulose materials (MacDonald et al. 2017). However, in this testing, the CMC fabric showed better hemostatic performance than the reference ORC material. Our experiment revealed the effective hemostatic activity of some newly developed materials. Carboxymethyl cellulose is a modified cellulose derivative. The process of carboxymethylation results in good water solubility or gelling properties depending on the degree of substitution (Aoshima et al. 2012; Ohta et al. 2015). Materials composed of sodium salt of carboxymethyl cellulose absorb blood, dissolve in it and affect the viscosity of blood. After this process, they interact with blood constituents and promote clotting (Ohta et al. 2015). CMC also specifically incorporates itself into the fibrin structure and increases the mechanical strength of the clot (Aoshima et al. 2012). The type of a material (regenerated/native cellulose), the degree of polymerization (DP - size of molecule), and the degree of substitution (DS) are essential for the hemostatic effect. Generally, the DS together with the molecular weight and porosity of a material play a main role towards final results. The water absorption may be decreased with a growing DS. Contrary to this fact, the increase of the DS may reflect a better dissolution. It is necessary to optimize the DS and thus achieve the best hemostatic effect. There are studies that suggest a moderate degree as the most appropriate (Ohta et al. 2015). Results of our study highlight the hemostatic efficiency of materials with DS around 0.7. These materials had more carboxyl groups, which in the presence of sodium salts dissociated, the materials gelled faster; they easily dissolved and could react with the blood. Materials of the same DS in their acidic form were more stable and did not dissociate. They only created dimers, which reflected in slower hemostasis. Fabrics based on CMC with lower DS were less soluble and less effective in hemostasis. As it turned out, the hemostatic ability went down also with the increasing free swell absorptive capacity. In the form of sponges, materials had the lowest free swell absorptive capacity. They gelled immediately and dissolved more rapidly. Free carboxyl groups were then more accessible for a possible interaction. On the other hand, more stable materials, which kept the shape longer, gelled only partly. The blood diffused through them and less of the functional groups reacted.

Specifically, the newer sponges and the knit consisting of carboxymethyl cellulose sodium salt showed required hemostatic potential; the other knit, in its acidic form, and nonwoven textiles were less effective. CMC Na sponge, CMC Na/Coll sponge and CMC Na knit effectively stopped the bleeding in less than 10 seconds. Time to hemostasis for the reference material was 3-4 times longer. The time necessary to stop blood loss was shorter also compared to the materials of other accessible studies (Chalupova et al. 2012; Yucel et al. 2016). A solid look on the oxidized cellulose and carboxymethyl cellulose processed into different forms enabled the complex evaluation of these derivatives. CMC Na sponge and CMC Na/Coll sponge reached the best hemostatic effect of all assessed groups. We attribute this fact to their structure. Both materials were lyophilized and prepared as sponges. One of the sponge's many benefits is its easy handling, so many surgeons prefer them (Fontes et al. 2018). Lyophilized products can dissolve more rapidly due to the faster liquid diffusion and after that, they actively facilitate clotting (Yan et al. 2017). The addition of collagen did not significantly improve the hemostatic effect. The ability to stop the bleeding of the two tested sponges was almost comparable. The product with collagen was a little less effective in hemostasis, because unlike the sodium salt of CMC, collagen was not that well soluble. Besides, the fabric with collagen was more irritable, which reflected in the worse histopathological evaluation. Carboxymethyl cellulose sodium salt in the form of a sponge was the most hydrophilic material in this assessment and had advantageous opportunity to stop bleeding, preferably by the formation of clotting

as well as by the interference with the attraction and aggregation of platelets. Its ability to combine both a physical and chemical mechanism guaranteed a significant effect. Moreover, the successful bioresorbability of the material was an essential and desirable finding. This further attribute allows the surgeon to leave the hemostatic dressing inside the body. Several materials with great hemostatic potential are inapplicable in surgery because of the non-bioresorbability (Achneck et al. 2010). Some manufacturers recommend the removal of the applied preparation once hemostasis is achieved. In fact, most of the materials are left on the wound to prevent postoperative bleeding (Lemoy et al. 2016). In case of non-bioresorbability, this solution may cause an undesirable irritation of the tissue and impair its regeneration. The extent of irritation may be influenced by the amount of material that has been used (Badenes et al. 2017).

Favorable hemostatic results and suitable structure properties reflected in the histopathological determination as well. Results of the 3-day assessment reflected the hemostatic ability. Results of the 30-day assessment were influenced by the structure, properties and behaviour of materials. Presence of inflammation is natural at the beginning of the healing process. After 30 days, an extensive inflammatory reaction represents an unfavorable aspect. The irritability of a material results in the creation of granulomas in the wound. The presence of a hematoma is common in the wound after surgery. These hematomas are usually absorbed within two weeks. Granulation accompanied by tissue formation, adequate scar formation and angiogenesis are desirable indications of healthy healing. Scarring is a natural part of the healing process. If some material impedes the normal process of healing, it may result in excessive scarring and the creation of dysfunctional tissue. Necrosis is also common after such an intervention, but the extent of necrosis is ultimately decisive. If the material does not work properly as a hemostatic tool, it causes extensive hemorrhaging, dystrophic changes, and tissue necrosis. The rate of destruction should correspond to the exact efficacy of the material. In the histopathological evaluation, the CMC Na sponge demonstrated the most favorable effect in each period of time. After 30 days, developed healing, characterized by regenerative and reparative processes in the renal parenchyma with only a light presence of inflammation, was noticed. On the other hand, the CMC Na/Coll sponge with similar hemostatic characteristics showed significant inflammatory response at the site of injury after 30 days. The reference ORC fibril had an undesirable effect on the tissue after a longer period of time. This could be a consequence of its fibrous structure. Fibers could be easily released into the wound and irritate the surroundings.

Very similar results could be seen in comparing the CMC H knit and PP/Vis needle-punched by looking at their quite favorable hemostatic activity and the final histopathological evaluation. Both materials were great hemostats in comparison with the reference material. Nevertheless, there was not such a significant difference that we could notice by using the above-mentioned sponges or CMC Na knit. The main difference between the CMC H knit and the PP/Vis needle-punched was in bioresorbability, which is derived from their structure. The knit was completely absorbed within 30 days. The viscose textile was not bioresorbable at all.

Contrary to the auspicious findings, two materials, the CMC Na needle-punched nonwoven textile and the CMC H spunlace, were less effective in the overall assessment. Materials proved perceptible hemostatic ability, but they were not bioresorbable, because of the lower DS and higher molecular weight. The acidic form of carboxymethyl cellulose in the CMC H spunlace, which should predetermine better hemostatic potential, did not live up to this potential. Nor did the histopathological evaluation turn out well for this material. The adverse effect on the tissue was most likely caused by loose fibers as well as the structural design as a whole.

Conclusions

In vivo experiments enabled the comparison of different structural materials based on carboxymethyl cellulose, oxidized cellulose, or viscose. Materials with higher degree of substitution provided faster hemostasis. When comparing the same DS, materials based on the sodium salt of carboxymethyl cellulose gelled faster and were more reactive than materials in their acidic form. When comparing the porosity and structure of materials with the same DS, sponges were more

effective in hemostasis than knits. Overall, nonwoven textiles of spunlace or needle-punched structure were less effective. Generally, the CMC proved better efficiency than oxidized cellulose or viscose. All in all, specifically, the CMC Na sponge proved to be a significantly more efficient hemostatic preparation in the overall assessment by reaching better results in all monitored parameters. The new preparation needed a shorter time to achieve hemostasis and showed itself to be bioresorbable and efficient in the regeneration of renal parenchyma. The final effect was influenced by the composition and structure together as a whole. In conclusion, we have brought forth a new material for human and veterinary use, which offers sufficient hemostatic activity, biocompatibility, bioresorbability, and easy manipulation. With such a valuable potential, it can be further refined and improved.

Declarations

ACKNOWLEDGEMENTS

This study was funded by the grant IGA VFU BRNO (322/2016/FaF) and solved with the financial support of TA ČR (TH04020540).

Conflicts of interest: The authors declare that they have no conflict of interest.

Availability of data and material: Not applicable

Code availability: Not applicable

Funding: This study was funded by the grant IGA VFU BRNO (322/2016/FaF) and covered by the project TAČR (TH04020540).

Authors' contributions: Conceptualization: [Pavel Suchý, Tomáš Sopuch, Lucy Vojtová]; Methodology: [Pavel Suchý, Lucy Vojtová]; Formal analysis and investigation: [Alice Paprskářová, Pavel Suchý, Marta Chalupová, Lenka Michlovská, Jarmila Klusaková, Lucy Vojtová]; Writing - original draft preparation: [Alice Paprskářová, Lenka Michlovská, Tomáš Sopuch, Lucy Vojtová]; Writing - review and editing: [Alice Paprskářová, Pavel Suchý, Marta Chalupová, Lenka Michlovská, Tomáš Sopuch, Lucy Vojtová]; Funding acquisition: [Alice Paprskářová, Pavel Suchý, Tomáš Sopuch, Lucy Vojtová]; Resources: [Pavel Suchý, Jarmila Klusáková, Tomáš Sopuch, Lucy Vojtová]; Supervision: [Pavel Suchý, Tomáš Sopuch, Lucy Vojtová].

References

1. Achneck HE, Sileshi B, Jamiolkowski RM, Albala DM, Shapiro ML, Lawson JH (2010) A comprehensive review of topical hemostatic agents: efficacy and recommendations for use. Ann surg 251:217-228. doi: 10.1097/SLA.0b013e3181c3bcca.
2. Aoshima M, Tanabe K, Kohno I, Jo Y, Takahashi K, Sugo T, Matsuda M (2012) Hemostatic mechanisms of a soluble fraction of plant-derived sodium carboxymethyl cellulose. Jpn J Thromb Hemost 23:387-398. doi: 10.2491/jjsth.23.387.
3. Badenes D, Pijuan L, Curull V, Sanchez-Font A (2017) A foreign body reaction to Surgicel® in a lymph node diagnosed by endobronchial ultrasound-guided transbronchial needle aspiration. Ann Thorac Med 12:55-56. doi: 10.4103/1817-1737.197780.
4. Centeno A, Rojas S, Arias B, Miquel I, Sánchez P, Ureta C, Rincón E, López R, Murat J (2020) Experimental Evaluation of a New Tissue Factor-Based Topical Hemostat (TT-173) for Treatment of Hepatic Bleeding. J Invest Surg 33:339-349. doi: 10.1080/08941939.2018.1517840.

5. Chalupová M, Suchý P, Pražanová G, Bartošová L, Sopuch T, Havelka P (2012) Local tissue reaction after the application of topical hemostatic agents in a rat partial nephrectomy model. J Biomed Mater Res Part A 100:1582-1590. doi: 10.1002/jbm.a.34098.
6. El-Sakhawy M, Milichovsky M (2000) Oxycellulose modification. Polym Int 49:839–844. doi: 10.1002/1097-0126(200008)49:8<839::AID-PI463>3.0.CO;2-T.
7. Fontes CER, Mardegam MJ, Prado-Filho OR, Ferreira MV (2018) Comparative analysis of surgical hemostatic sponges in liver injury: study in rats. ABCD Arq Bras Cir Dig 31:e1342. doi: 10.1590/0102-672020180001e1342.
8. Fukuzumi H, Saito T, Okita Y, Isogai A (2010) Thermal stabilization of TEMPO-oxidized cellulose. Polym Degrad Stab 95:1502-1508. doi: 10.1016/j.polymdegradstab.2010.06.015.
9. Hassouna HA, Manikandan R (2012) Hemostasis in laparoscopic renal surgery. Indian J Urol 28:3-8. doi: 10.4103/0970-1591.94939.
10. Huri E, Akgul T, Ayyildiz A, Ustun H, Germiyanoglu C (2009) Hemostatic role of a folkloric medicinal plant extract in a rat partial nephrectomy model: controlled experimental trial. J Urol 181:2349-2354. doi: 10.1016/j.juro.2009.01.016.
11. Ikehara S, Sakakita H, Ishikawa K, Akimoto Y, Yamaguchi T, Yamagishi M, Kim J, Ueda M, Ikeda JI, Nakanishi H, Shimizu N, Hori M, Ikehara Y (2015) Plasma blood coagulation without involving the activation of platelets and coagulation factors. Plasma Process Polym 12:1348-1353. doi: 10.1002/ppap.201500132.
12. Lemoy MMF, Schouten AC, Canfield DR (2016) Granuloma Due to Oxidized Regenerated Cellulose in an Aged Rhesus Macaque (Macaca mulatta). Comp Med 66:59-62.
13. MacDonald MH, Wang AY, Clymer JW, Hutchinson RW, Kocharian R (2017) An in vivo comparison of the efficacy of hemostatic powders, using two porcine bleeding models. Med Devices 10:273-279. doi: 10.2147/MDER.S140663.
14. Ohta S, Nishiyama T, Sakoda M, Machioka K, Fuke M, Ichimura S, Inagaki F, Shimizu A, Hasegawa K, Kokudo N, Kaneko M, Yatomi Y, Ito T (2015) Development of carboxymethyl cellulose nonwoven sheet as a novel hemostatic agent. J Biosci Bioeng 119:718-723. doi: 10.1016/j.jbiosc.2014.10.026.
15. Ozgor F, Simsek A, Aydogdu O, Kucuktopcu O, Sarilar O, Berberoglu AY, Akbulut MF, Binbay M (2016) Bleeding during laparoscopic partial nephrectomy: Can a hemostatic matrix help to improve hemostasis?. Arch Ital Urol Androl 88:228-232. doi: 10.4081/aiua.2016.3.228.
16. Panwar V, Thomas J, Sharma A, Chopra V, Kaushik S, Kumar A, Ghosh D (2020) In-vitro and in-vivo evaluation of modified sodium starch glycolate for exploring its haemostatic potential. Carbohydr Polym 235:115975. doi: 10.1016/j.carbpol.2020.115975.
17. Samudrala S (2008) Topical hemostatic agents in surgery: a surgeon's perspective. AORN J 88:s2-11. doi: 10.1016/S0001-2092(08)00586-3.
18. Schonauer C, Tessitore E, Barbagallo G, Albanese V, Moraci A (2004) The use of local agents: bone wax, gelatin, collagen, oxidized cellulose. Eur Spine J 13:89-96. doi: 10.1007/s00586-004-0727-z.
19. Slezak P, Keibl C, Labahn D, Schmidbauer A, Genyk Y, Gulle H (2020) A Comparative Efficacy of Recombinant Topical Thrombin (RECOTHROM®) With A Gelatin Sponge Carrier Versus Topical Oxidized Regenerated Cellulose (TABOTAMP®/SURGICEL®) In a Porcine Liver Bleeding Model. J Invest Surg 1-7. doi: 10.1080/08941939.2019.1705444.
20. Song H, Zhang L, Zhao X (2010) Hemostatic efficacy of biological self-assembling peptide nanofibers in a rat kidney model. Macromol Biosci 10:33-39. doi: 10.1002/mabi.200900129.
21. Spangler D, Rothenburger S, Nguyen K, Jampani H, Weiss S, Bhende S (2003) In vitro antimicrobial activity of oxidized regenerated cellulose against antibiotic-resistant microorganisms. Surg Infect (Larchmt) 4:255-262. doi: 10.1089/109629603322419599.

22. Suchý P, Paprskářová A, Chalupová M, Marholdová L, Nešporová K, Klusáková J, Kuzmínová G, Hendrych M, Velebný V (2020) Composite Hemostatic Nonwoven Textiles Based on Hyaluronic Acid, Cellulose, and Etamsylate. Materials (Basel) 13:1627. doi: 10.3390/ma13071627.
23. Wang J, Somasundaran P (2005) Adsorption and conformation of carboxymethyl cellulose at solid-liquid interfaces using spectroscopic, AFM and allied techniques. J Colloid Interf Sci 291:75–83. doi: 10.1016/j.jcis.2005.04.095.
24. Wu Y, Wang F, Huang Y. Comparative Evaluation of Biological Performance, Biosecurity, and Availability of Cellulose-Based Absorbable Hemostats (2018) Clin Appl Thromb Hemost 24:566-574. doi: 10.1177/1076029617751177.
25. Yan T, Cheng F, Wei X, Huang Y, He J (2017) Biodegradable collagen sponge reinforced with chitosan/calcium pyrophosphate nanoflowers for rapid hemostasis. Carbohydr Polym 170:271-280. doi: 10.1016/j.carbpol.2017.04.080.
26. Yucel MO, Polat H, Bagcioglu M, Karakan T, Benlioglu C, Cift A, Gok A, Astarci HM, Akgul T, Germiyanoglu C (2016) Comparison of the efficacy and histopathological effects of three hemostatic agents in a partial nephrectomy rat model. Int Urol Nephrol 48:65-71. doi: 10.1007/s11255-015-1129-3.
27. Zhang S, Li J, Chen S, Zhang X, Ma J, He J (2020) Oxidized cellulose-based hemostatic materials. Carbohydr Polym 230:115585. doi: 10.1016/j.carbpol.2019.115585.

Figures

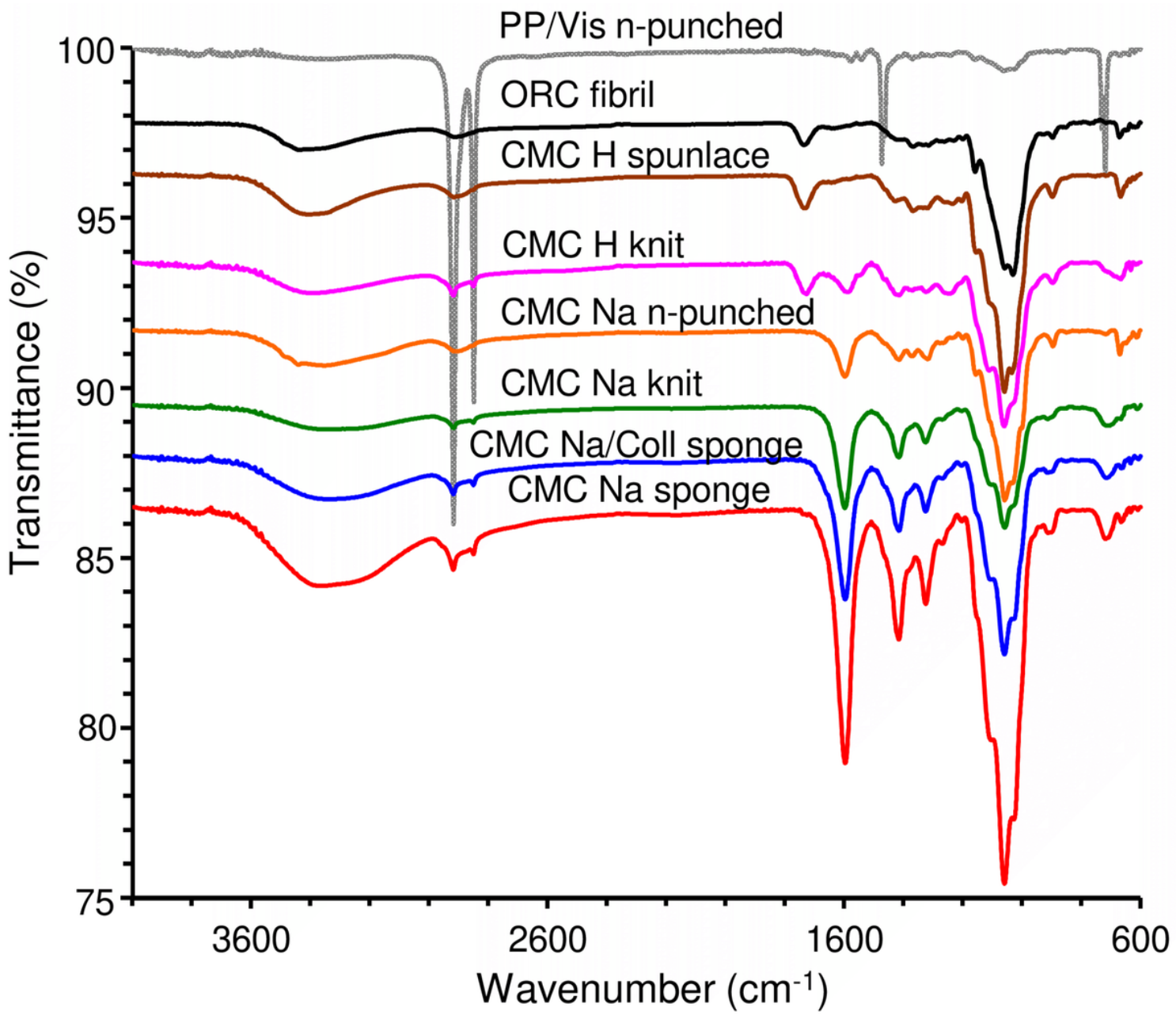

Figure 1

ATR-FTIR spectra of different hemostatic samples

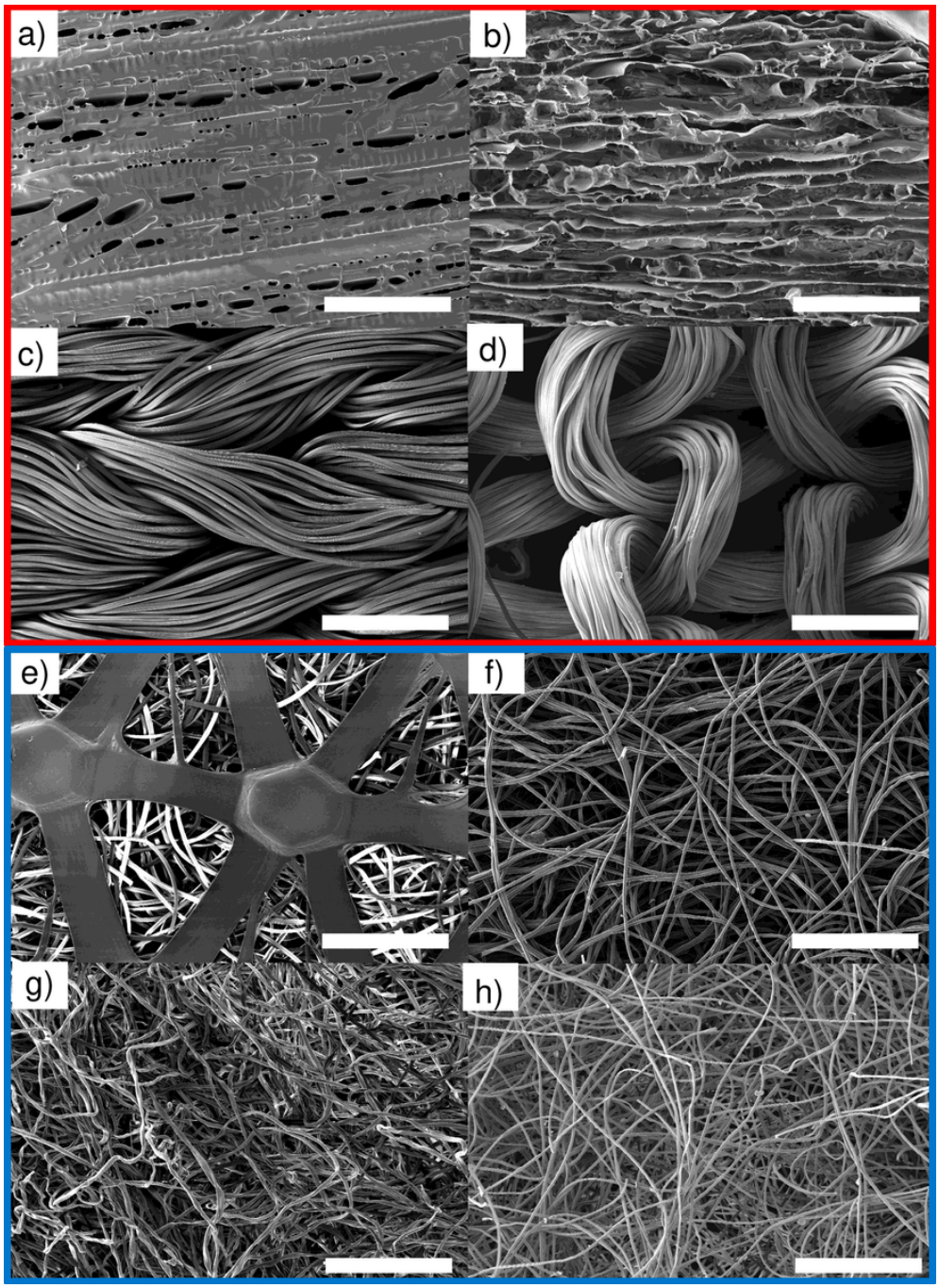

Figure 2

Morphology of hemostatic materials. Magnification 150×, scale bars represent 500 μm, a) CMC Na sponge, b) CMC Na/Coll sponge, c) CMC Na knit, d) CMC H knit, e) PP/Vis needle-punched, f) CMC Na needle-punched, g) CMC H spulance, h) ORC fibril.

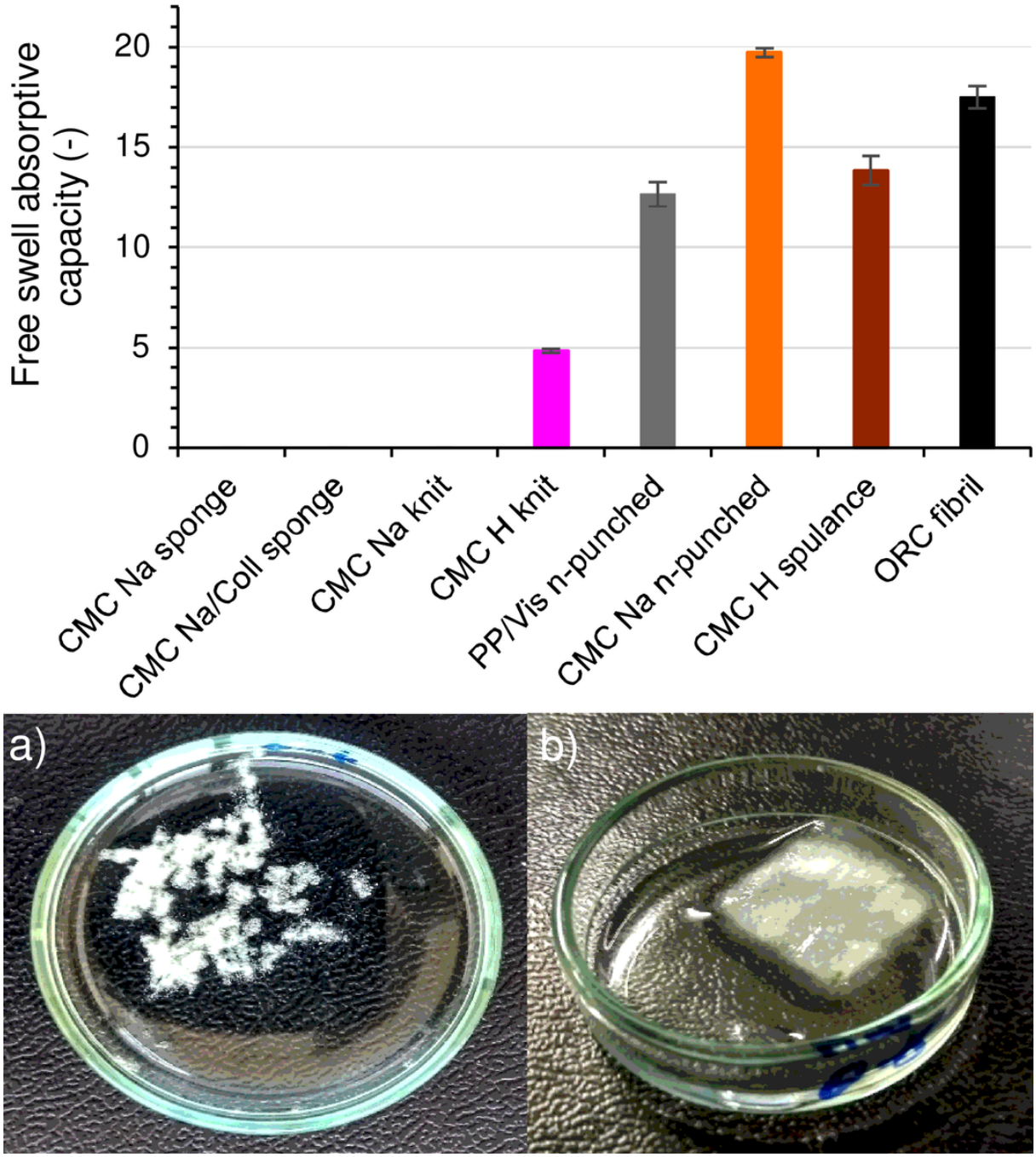

Figure 3

Free swell absorptive capacity of hemostatic materials. Values represent the means ± S.D. of 5 determinations. a) CMC Na sponge after addition of the solution, the lowest ratio; b) CMC Na needle-punched after addition of the solution, the highest ratio

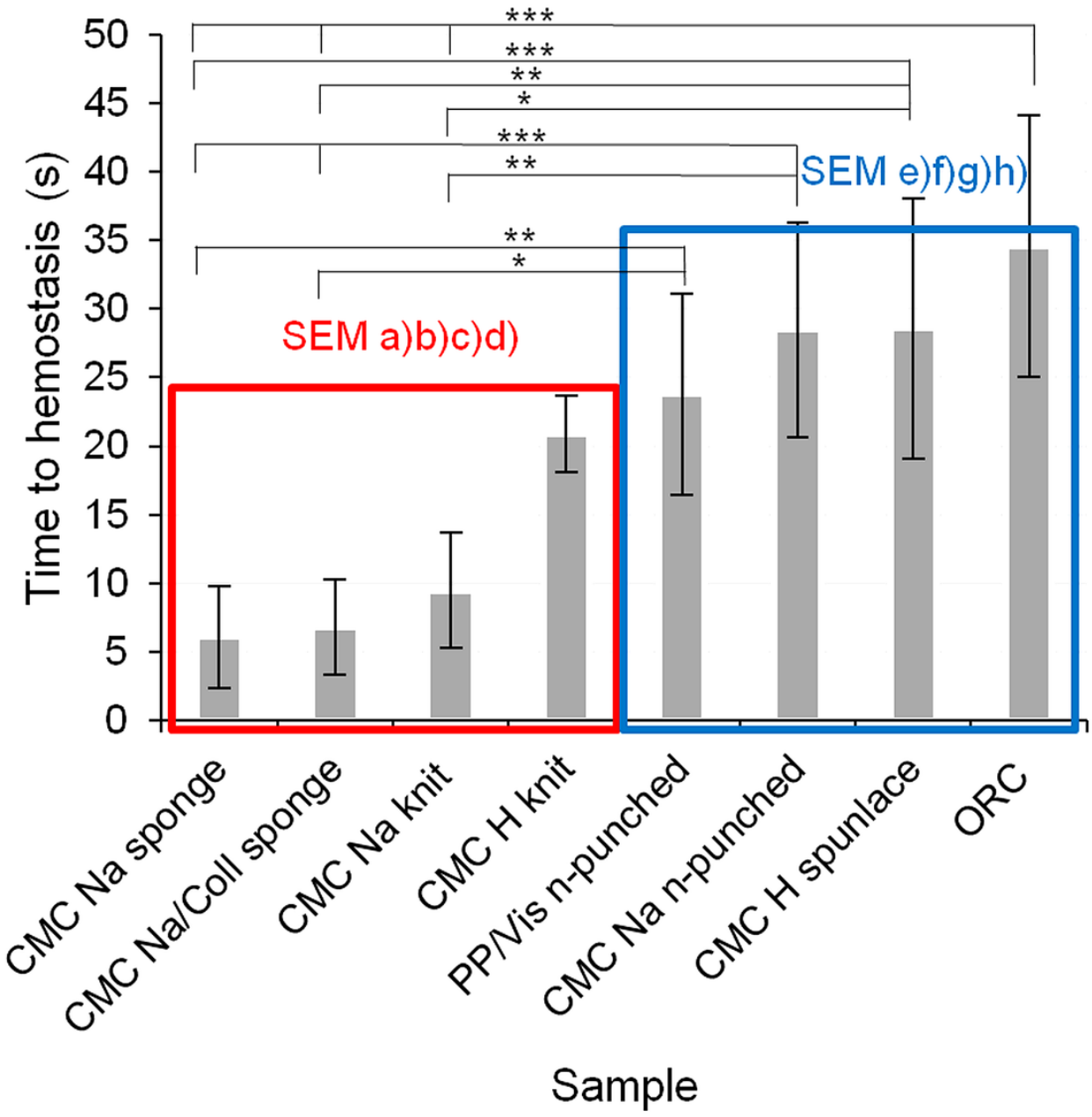

Figure 4

Time to hemostasis in seconds. Values represent the means ± S.D. of 10 determinations. * $p < 0.05$, ** $p < 0.01$, *** $p < 0.001$ in mutual comparison. Samples with red edging correspond to SEM images a)b)c)d) and samples with blue edging correspond to SEM images e)f)g)h).

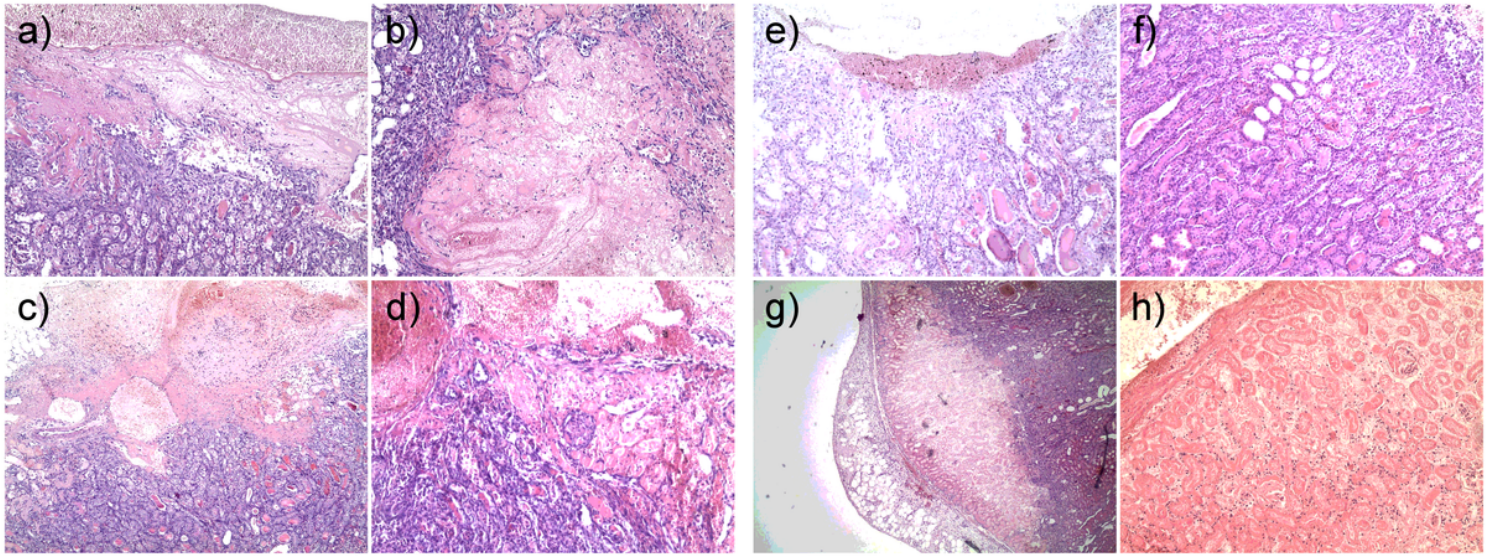

Figure 5

Histological images after 3 days, H&E. a) CMC Na sponge: Magnification 100×; zone of necrosis, zone of inflammation. b) CMC Na/Coll sponge: Magnification 100×; massive inflammation, necrosis. c) CMC Na knit: Magnification 50×; necrotic tissue, renal tubules with a massive inflammation around. d) CMC H knit: Magnification 100×; clear destruction of the tissue by necrosis, bleeding, massive inflammation. e) PP/Vis needle-punched: Magnification 100×; smooth cutting line with hematoma, protein cylinders with significant reaction. f) CMC Na needle-punched: Magnification 100×; close-up shot of the damaged tissue with protein cylinders, bruised edge next to the cutting line, sign of fibroproduction. g) CMC H spunlace: Magnification 25×; presence of necrosis, inflammatory reaction. h) Control ORC fibril: Magnification 100×; necrotic tissue, inflammatory infiltrate.

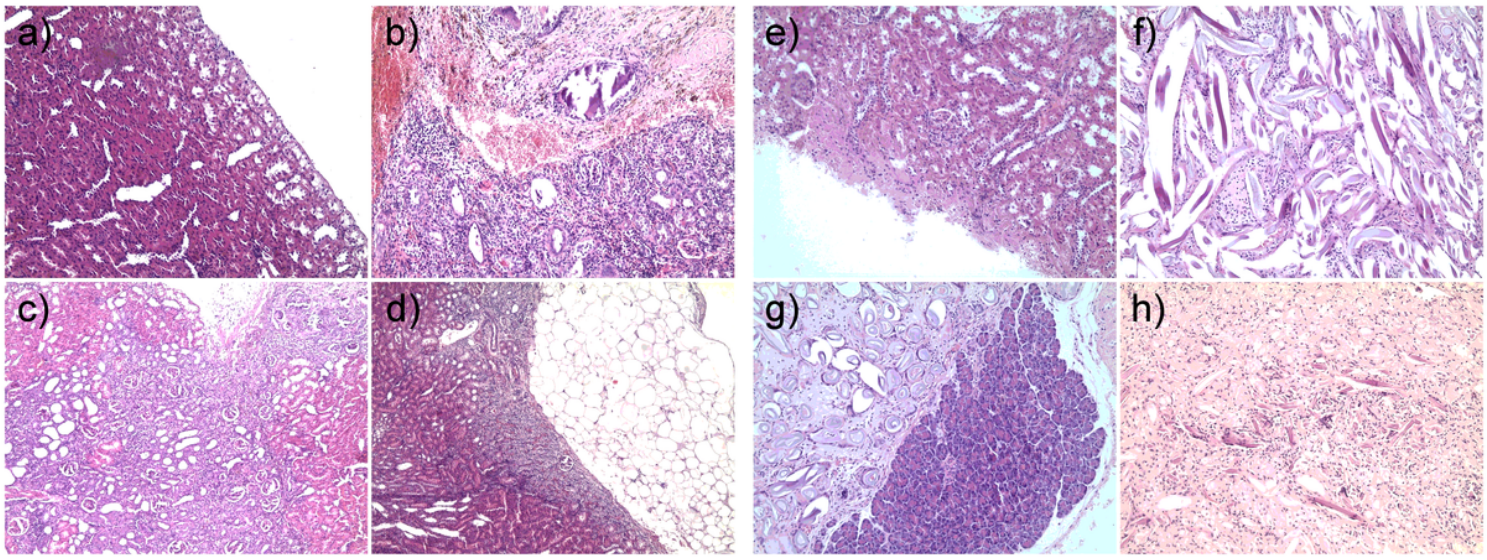

Figure 6

Histological images after 30 days, H&E. a) CMC Na sponge: Magnification 100×; almost clear cutting line with only temperate inflammation and light regression. b) CMC Na/Coll sponge: Magnification 100×; presence of granulomas, bleeding, the zone of inflammation. c) CMC Na knit: Magnification 50×; significant inflammation, granulomas. d) CMC H knit: Magnification 50×; relatively narrow zone of the inflammation. e) PP/Vis needle-punched: Magnification 100×; minimal inflammatory reaction, little scarring. f) CMC Na needle-punched: Magnification 100×; close-up shot of a rest of the material, inflammatory reaction with significant scarring. g) CMC H spunlace: Magnification 100×; rest of the

material, forming of a scar tissue. h) Control ORC fibril: Magnification 100×; granuloma around the foreign material, chronic inflammatory infiltrate.